U.P.B. Sci. Bull., Series C, Vol. 76, Iss. 4, 2014 ISSN 2286-3540

ON THE ESTIMATION OF INTRINSIC DIMENSION FOR 3D IMAGES

Serban Oprisescu[1], Monica Dumitrescu[2]

The paper deals with the estimation of intrinsic dimension (ID) for three dimensional images produced by different cameras such as a time-of-flight (ToF), Kinect or other sensors. We introduce a slightly different definition (ID_S) allowing the use of samples extracted from the contours within images. We have implemented the maximum likelihood estimator based on a fixed number of sub-spheres. The experimental study we perform compares the performances of the estimated ID for intensity (2D) ToF images and distance (3D) ToF images. Based on this comparison, one could use ID appropriately in a fusion system for images provided by two-dimensional and three dimensional sensors.

Keywords: Intrinsic dimension, Maximum likelihood estimate, Local structure

1. Introduction

In signal processing, the intrinsic dimensionality (ID) of a signal describes how many variables are needed to represent that signal, and it is a key priori knowledge to improve performance of processing. A reduction of the dimension can result in reduced computational time, as the use of more dimensions than strictly necessary leads to several problems such as the space needed to store the data, compression for storage purposes, the speed of algorithms ([1]).

The analysis of local image regions which contain lines or edges became an issue of genuine interest in early 80's and it is the paper of Zetzsche and Barth (1990) [2] where the term "intrinsic dimension" was introduced. According to this approach, intrinsic dimension of an image f has been defined for open, convex regions $\Omega \subset R^p$, $p \geq 2$, and it has been denoted $ID_\Omega(f)$. Important related results have followed, such as the uniqueness proof (Mota and Barth (2000) [3]), the extensions to multiple orientations (Aach et al (2006) [4]), the application for multiple motions (Mota et al (2001) [5]) and the extensions to multispectral signals (Mota et al (2006) [6]).

On the other hand, there exist some other approaches of the ID issue, such as the one in [7] but, for the time being, we've started from the original definition of $ID_\Omega(f)$.

[1]Lecturer, Image Processing and Analysis Laboratory, University POLITEHNICA of Bucharest, Romania, e-mail: soprisescu[adt]imag.pub.ro

[2]Professor, Faculty of Mathematics and Computer Science, University of Bucuresti, Romania

In practice, any definition of ID must be accompanied by an estimation procedure. ID estimation methods can be classified into three groups: projection approach, geometric approach and probabilistic (or statistical) approach. *The projection approach* first projects data into a low-dimensional space and then determine the ID by verifying the low-dimensional representation of data (PCA is a classical projection method). *Geometric approaches* make use of the geometric structure of data to build ID estimators (fractal-based methods have been well developed and used in time series analysis). *The probabilistic technique* builds estimators by making distribution assumptions on data. The maximum likelihood (MLE) method proposed by Levina and Bickel (2004) [8] is a representative method of this approach, whose final global estimator is given by averaging the local estimators. MacKay and Ghahramani (2005) [9] pointed out that, compared with averaging the local estimators directly, it is more sensible to average their inverses for the maximum likelihood purpose. Multiple applications of local intrinsic dimension estimation are discussed by Carter et al ([10]). An experimental approach of estimating the intrinsic dimension using inherent clustering present in data is discussed by Eriksson and Crovella ([11]).

In this paper we adopt a statistical approach for both the definition and the estimation of ID and present an experimental study which compares two ways of computing the intrinsic dimension of (depth) image structures.

- By defining and estimating intrinsic dimension locally, we can experimentally prove the efficiency of ID to identify local structures (lines, edges, corners).
- By analyzing 2D images versus 3D ToF images, we offer a possible way for superimposing / fusing 2D with depth information.

We modify the classical definition of intrinsic dimension of an image f, in such a way that it is directly connected to a sample $S = \{\overrightarrow{v_1}, ..., \overrightarrow{v_n}\}$ (where the $\overrightarrow{v}'s$ are the position vectors of the sample points) from that structure and we denote the intrinsic dimension with respect to a sample S by $ID_S(f)$. Afterwards, we apply the MLE method in order to estimate $ID_S(f)$.

The paper focusses on three dimensional images produced by a time-of-flight (ToF) camera but, of course, other sensors could be considered too. Some substructures in the image may be viewed as structures in a two dimensional space too. Therefore, one would be interested in comparing the performances of ID's as *diagnosis tools* in $2D$ and $3D$ cases. We implement the maximum likelihood estimation of ID_S for two dimensional (photo) images and for three dimensional images produced by a ToF camera. The experimental study we perform aims at establishing a comparison of the performances of the estimator in the case of different dimensional images. Our conclusion is that the estimated $ID_S(f)$ can be used appropriately in a fusion system for images provided by two-dimensional and three dimensional sensors ([12]).

2. ID_S definition and estimation

Let us consider a $3D$ image defined by a probability density f on the measurable set $(R^3, \mathcal{B}^3)$, where $\mathcal{B}^3$ is the Borel σ field, and let $S = \{\overrightarrow{v_1}, ..., \overrightarrow{v_n}\} \subset R^3$ be a sample of **available observations**, which are independent, identical distributed random vectors. Assume there exist $m \leq 3$ and the following items:

• $\{\overrightarrow{u_1}, ..., \overrightarrow{u_n}\} \subset R^m$, independent, identical distributed random vectors with a probability density $g(\overrightarrow{u})$ on R^m,

• a matrix $B(3,m)$, such that $\overrightarrow{v_i} = B\overrightarrow{u_i}$, $i = 1, ..., n$

Hence, $\overrightarrow{v_1}, ..., \overrightarrow{v_n}$ are independent, identical distributed random vectors with a probability density denoted $f(\overrightarrow{v})$, which can be calculated from $g(\overrightarrow{u})$.

Then, the smallest number m for which the above property holds is called the *intrinsic dimension associated with the probability density f and the sample* $S = \{\overrightarrow{v_1}, ..., \overrightarrow{v_n}\}$ and it is denoted $ID_S(f)$. We have $0 \leq ID_S(f) \leq 3$.

Comment:

If $ID_S(f) = 0$, then f is constant for the sample $\{\overrightarrow{v_1}, ..., \overrightarrow{v_n}\}$ with respect to all three variables (no local structure). If $ID_s(f) = 1$, then f varies for the sample $\{\overrightarrow{v_1}, ..., \overrightarrow{v_n}\}$ along one direction (a curve, an edge). If $ID_S(f) = 2$, then f varies for the sample $\{\overrightarrow{v_1}, ..., \overrightarrow{v_n}\}$ along two directions (a surface, a plane). If $ID_S(f) = 3$, then f varies for the sample $\{\overrightarrow{v_1}, ..., \overrightarrow{v_n}\}$ with respect to all three variables (a corner).

A similar definition for a two-dimensional image and a sample S can be considered, and the corresponding discussion is: if $ID_S(f) = 0$, then f is constant for the sample $\{\overrightarrow{v_1}, ..., \overrightarrow{v_n}\}$ with respect to both variables (no local structure). If $ID_S(f) = 1$, then f varies for the sample $\{\overrightarrow{v_1}, ..., \overrightarrow{v_n}\}$ along one direction (a curve, a line). If $ID_S(f) = 2$, then f varies for the sample $\{\overrightarrow{v_1}, ..., \overrightarrow{v_n}\}$ with respect to both variables (a corner).

To estimate $ID_S(f)$, we proceed from the MLE proposed by Levina and Bickel (2004) and commented by MacKay and Ghahramani (2005). The basic ideas of this approach are the following: (a) one can introduce an approximation of the volume of the $j-$th nearest neighbor sphere by means of a counting process; (b) the counting process can be approximated by a inhomogeneous Poisson process and its intensity can be estimated by the maximum likelihood method.

Let us consider a set of random vectors $S = \{\overrightarrow{v_1}, ..., \overrightarrow{v_n}\} \subset R^p$ ($p = 2$ or 3) and assume that m is the true, unknown intrinsic dimension associated with the density $f(\overrightarrow{v})$ and this sample. Let $V_r(m)$ denote the volume of the sphere with radius r, in R^m. Then $V_r(m) = V(m) \cdot r^m$, where $V(m)$ denotes the volume of the unit sphere in R^m. For $\overrightarrow{v_{i_0}}$ fixed, let $T_j(\overrightarrow{v_{i_0}})$ denote the Euclidean distance from $\overrightarrow{v_{i_0}}$ to its $j-$th nearest neighbor (NN) in the set and let $S(\overrightarrow{v_{i_0}}; T_j(\overrightarrow{v_{i_0}}))$ denote the $j-$NN sphere around $\overrightarrow{v_{i_0}}$. The proportion of sample points falling into the $j-$NN sphere around $\overrightarrow{v_{i_0}}$ is roughly $f(\overrightarrow{v_{i_0}})$ times the volume of the sphere, $j/n \simeq f(\overrightarrow{v_{i_0}}) \cdot V(m) (T_j(\overrightarrow{v_{i_0}}))^m$.

The sample $S = \{\overrightarrow{v_1}, ..., \overrightarrow{v_n}\}$ is obtained by means of a count process. We recall that a stochastic process $\{N(t), t \in [0, \infty)\}$ is called a *count process* (or an *arrival process*) if it is a jump - process (it increases by jumps only), $N(0) = 0$, and its trajectories are non-decreasing, right - continuous functions. A count process is called a *Poisson process* if the range of its jumps is equal to 1, $(N(s+t)-N(s))$ is independent of $\{N(u), u \leq s\}$, and the distribution of $(N(s+t)-N(s))$ is independent of s. Observation of a Poisson process can be continuously performed, either over a fixed period $[0,T]$ or over a random period, until N_0 arrivals occur.

Applying these facts for images in R^p ($p = 2$ or 3) with ID equal to m (unknown), we have the parameter $r \in [0,\infty)$ and the count process addresses the spheres $S(\overrightarrow{v};r)$.

Based on Levina and Bickel approach, we assume that, for a fixed point $\overrightarrow{v}$, the image is characterized by a constant probability density $f(\overrightarrow{v}) \simeq ct$ in a small sphere with radius r around $\overrightarrow{v}$. Denote the number of observations within distance r from $\overrightarrow{v}$ by $N(\overrightarrow{v};r) = \sum_{i=1}^{n} 1_{\{\overrightarrow{v_i} \in S(\overrightarrow{v};r)\}}$

For a given $\overrightarrow{v}$, the inhomogeneous process $\{N(\overrightarrow{v};r), r \in [0,\infty)\}$ can be approximated by a inhomogeneous Poisson process. Suppressing the dependence on $\overrightarrow{v}$, we use the notation $\{N(r), r \in [0,\infty)\}$, and denote the intensity of this process by $\lambda(r)$. From the Poisson processes properties, the intensity (rate) is $\lambda(r) = \frac{d}{dr}(f(\overrightarrow{v}) \cdot V(m) r^m) = f(\overrightarrow{v}) \cdot V(m) m r^{m-1}$.

As we've mentioned, *estimation of m* can be achieved through two different approaches: (a) Consider $\{N(r), 0 \leq r \leq R\}$ and take into consideration the observations within the $j-$NN spheres, with $T_j(\overrightarrow{v}) \leq R$; (b) Consider a fixed number of $j-$NN, $j \leq J$ and take into consideration the observations for distances $\{T_j(\overrightarrow{v}),\ j \leq J\}$. In both cases, one would estimate the intensity of the Poisson process by the maximum likelihood method.

Case (a) (fixed maximum radius R)

The Levina & Bickel estimator for a fixed $\overrightarrow{v}$ is

$$\widehat{m_R}(\overrightarrow{v}) = \left(\frac{1}{N(\overrightarrow{v};R)} \sum_{j=1}^{N(\overrightarrow{v};R)} \log \frac{R}{T_j(\overrightarrow{v})} \right)^{-1} \tag{1}$$

The independent, identical distributed observations $\{\overrightarrow{v_1}, ..., \overrightarrow{v_n}\}$ represent an embedding of a lower dimensional sample $\{\overrightarrow{u_1}, ..., \overrightarrow{u_n}\}$.

- For any fixed point $\overrightarrow{v}$, consider a small sphere of radius R , consider the $j-$NN $j = 1,2,...$, and count the observations within the corresponding sub-spheres $S(\overrightarrow{v};T_1(\overrightarrow{v})) \subset S(\overrightarrow{v};T_2(\overrightarrow{v})) \subset ... \subset S(\overrightarrow{v};R)$. Accordingly, record the values $\{N(\overrightarrow{v};T_1(\overrightarrow{v})), N(\overrightarrow{v};T_2(\overrightarrow{v})), ..., N(\overrightarrow{v};R)\}$. *The radius R is fixed, but the number of sub-spheres in not fixed a priori.*
- Repeat the procedure for every observation $\overrightarrow{v_1}, ..., \overrightarrow{v_n}$ and calculate $\widehat{m_R}(\overrightarrow{v_i})$, $i = 1, ..., n$, using formula (1). Then, estimate the ID by

$$\widehat{m_R} = \frac{1}{n} \sum_{i=1}^{n} \widehat{m_R}(\overrightarrow{v_i}) \tag{2}$$

The modified MacKay and Ghahramani estimate is

$$\widehat{m_R}^{-1} = \left(\sum_{i=1}^{n} \sum_{j=1}^{N(\overrightarrow{v_i};R)} \log \frac{R}{T_j(\overrightarrow{v_i})} \right) / \left(\sum_{i=1}^{n} N(\overrightarrow{v_i};R) \right) \tag{3}$$

Case (b) (fixed number of NN-neighbours J)
The Levina & Bickel estimate for a fixed $\overrightarrow{v}$ is

$$\widehat{m_J}(\overrightarrow{v}) = \left(\frac{1}{J-1} \sum_{j=1}^{J-1} \log \frac{T_J(\overrightarrow{v})}{T_j(\overrightarrow{v})} \right)^{-1} \tag{4}$$

• For any fixed point $\overrightarrow{v}$, consider a small sphere of radius R , consider the $j-$NN $j = 1,2,...$, and count the observations within the corresponding sub-spheres $S(\overrightarrow{v};T_1(\overrightarrow{v})) \subset S(\overrightarrow{v};T_2(\overrightarrow{v})) \subset ... \subset S(\overrightarrow{v};T_J(\overrightarrow{v}))$. Accordingly, record the values $\{N(\overrightarrow{v};T_1(\overrightarrow{v})), N(\overrightarrow{v};T_2(\overrightarrow{v})), ..., N(\overrightarrow{v};T_J(\overrightarrow{v}))\}$. *The number of sub-spheres is fixed a priori.*

• Repeat the procedure for every observation $\overrightarrow{v_1},...,\overrightarrow{v_n}$ and calculate $\widehat{m_J}(\overrightarrow{v_i})$, $i = 1,...,n$, using formula (4) (or the one obtained by dividing by $(J-2)$). Then, estimate the ID by

$$\widehat{m_J} = \frac{1}{n} \sum_{i=1}^{n} \widehat{m_J}(\overrightarrow{v_i}) \tag{5}$$

The modified MacKay and Ghahramani estimate is

$$\widehat{m_J}^{-1} = \left(\sum_{i=1}^{n} \sum_{j=1}^{J-1} \log \frac{T_J(\overrightarrow{v_i})}{T_j(\overrightarrow{v_i})} \right) / (n \cdot (J-1)) \tag{6}$$

According to MacKay and Ghahramani , the modified estimates are less biased than the original Levina and Bickel ones.

3. Experimental Study

3.1. Methodology

We have conducted an experimental study to estimate $ID_S(f)$ for $2D$ images (either photo images, or intensity ToF images) and for $3D$ images (distance ToF images). In the case of $ID_S(f)$, we have used *samples* S extracted from the the contours within images (a sample represents a connected contour segment within the neighborhood). The performances of the estimates have been evaluated and a comparison of ID estimates for $2D$ and $3D$ images has been established.

- *A preliminary analysis* was performed on $2D$ natural images in order to choose between the estimators given by formulae (5) and (6). The conclusion was that formula (5) gives a stronger ID response than formula (6). Therefore, formula (5) was used in this study for estimating ID.

- We have focused our study on *local structures* such as $2D$ straight lines and $3D$ edges, $2D$ and $3D$ corners, connections or curved lines, as well as for planes in $3D$.

- In order to compute $ID_S(f)$, a contour extractor has been implemented and, afterwards, a sample set S was chosen (S represents the longest connected contour line within the current neighborhood). The obtained ID_S images are presented and interpreted and some key points are selected. The Canny extractor was used for $2D$ images, and an original contour extractor which works better than the Canny extractor was used for distance ToF images.

3.2. Reported results

Several images have been analyzed, and here we present the results for two images: a $2D$ natural, photo image (Fig. 1.a) and a ToF image (Fig. 1.b: intensity ToF image and Fig. 1.c: distance ToF image).

(A) (B) (C)

FIG. 1. a) Classic gray level test 2D-image "house.png"; b) Intensity ToF image; c) Distance ToF image

3.2.1. *$ID_S(f)$ for a $2D$ natural image.* The study addresses the image in Fig. 1.a. In order to obtain the "available observations", we have used the Canny contour extractor. Then, formula (5) has been implemented to estimate ID in specified pixels.

Fig. 2 displays the estimated $ID_S(f)$ on using formula (5). The $ID_S(f)$ is displayed as a level of gray, white meaning zero $ID_S(f)$ values (disregarded pixels) and black meaning the maximum obtained $ID_S(f)$ value. The overall maximum $ID_S(f)$ for the image in Fig. 1 was 1.67 (sky disregarded). Detailed ID values are included in Fig. 3.a - 3.g .

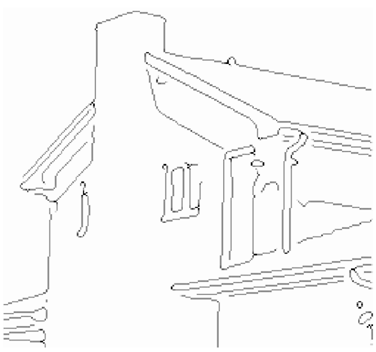

FIG. 2. ID_S image for the 2D image "house.png"

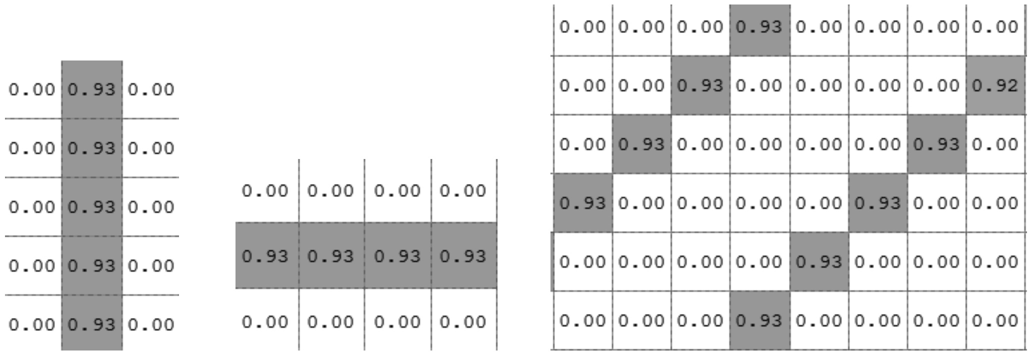

(A) (B) (C)

FIG. 3. Detailed ID_S values for straight lines

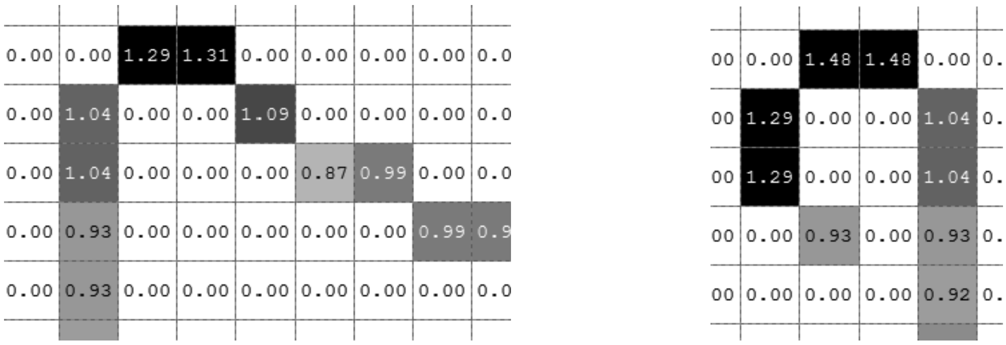

(D) (E)

FIG. 3. Detailed ID_S values for corners

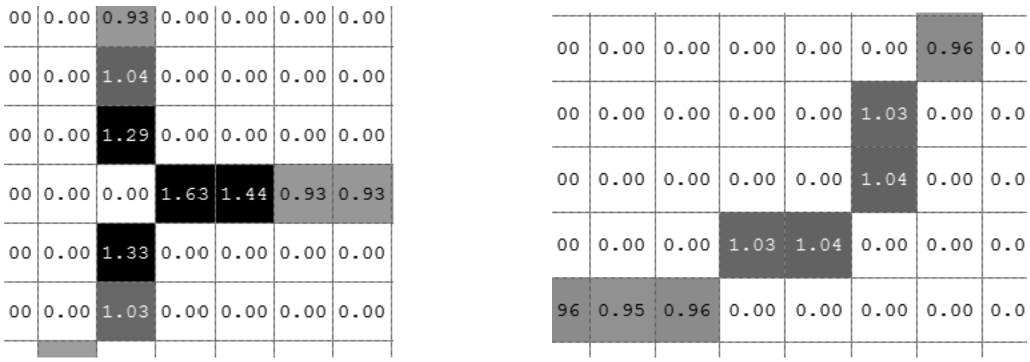

(F) (G)

FIG. 3. Detailed ID_S values for a connection point (f) and a low curvature corner (g)

• The $ID_S(f)$ values obtained for straight lines (at any orientation) are around 0.93, including the left side of the chimney, as shown in Fig. 3.a., b. and c. This result is conform to the theory (for a line the ID should be 1).

• In Fig. 3.d., the maximum value for a simple corner is around 1.3, while in Fig. 3.e., a strong curvature corner has an ID_S of 1.48 (should be 2). Fig. 3.g. shows that even a low curvature corner can be detected, the computed ID_S being grater than 1.

• In Fig. 3.f an example of connection point is shown. These points have the maximum ID_S over the whole image (sky disregarded).

We have considered the average values of the estimated $ID_S(f)$'s for some local patterns in order to check the efficiency of their (correct) identification.

In Table 1 we present the $2D$-ID values obtained for a specified ideal structure. The "max ID_S" value represents the maximum value on a pixel within the structure and the "average ID_S" represents the arithmetic mean over all pixels of the structure (the structure has about 5 to 9 pixels).

Table 1

$2D$ - ID_S values obtained for a specified ideal structure

2D structure	max ID_S	average ID_S
—	0.93	0.93
└	1.17	1.14
⊥	1.54	1.31
+	1.52	1.46
╕	1.78	1.45

Usually the maximum ID_S value is reached in the pixel where there are some crossing lines, but this value can be located also in the neighbor pixel, due to the fact that the ID_S is computed within a neighborhood. But, even if we don't obtain the absolute maximum in the theoretical point, this maximum is not farther than a pixel distance.

3.**2**.2. *$ID_S(f)$ for a ToF natural image.* The study addresses the images in Fig. 1.b and 1.c. We have used an original contour extractor, which searches for maximum curvature points within the distance image, as a deviation from linearity. This extractor works better than the Canny extractor for ToF distance images ([13]). Afterwards, formula (5) has been implemented to estimate the ID_S.

Fig. 4.a and 4.b display the ID_S image for intensity ToF image and ID_S image for distance ToF image respectively. As before, white stands for 0 ID (disregarded pixels) and black means maximum ID.

In Fig. 5.a - 5.h. the detailed ID_S values in the distance $(3D)$ ToF image are included: for $2D$ lines and corners, for $3D$ corners.

• If the sample S is extracted from a $2D$ line within a $3D$ image, the ID_S is between 0.93 and 0.98 (it should be 1).

• In Fig. 5.c one can see the distance profile of a corner in $2D$ (the upper plane is perpendicular to the ToF camera plane, and the corner is marked with a bright circle). The corresponding computed ID_S's are presented in Fig. 5.d. Thus, if S is extracted for a $2D$ corner within a $3D$ image, the ID_S is between 1 and 2 (it should be 2).

FIG. 4. a ,b: ID_S images for intensity / distance ToF image

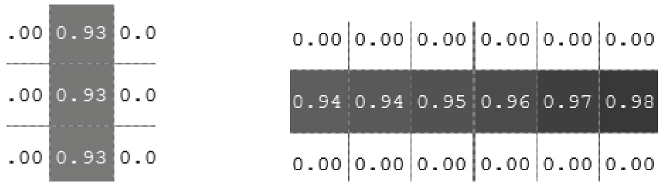

(A) (B)

FIG. 5. Detailed ID_S values for 2D lines

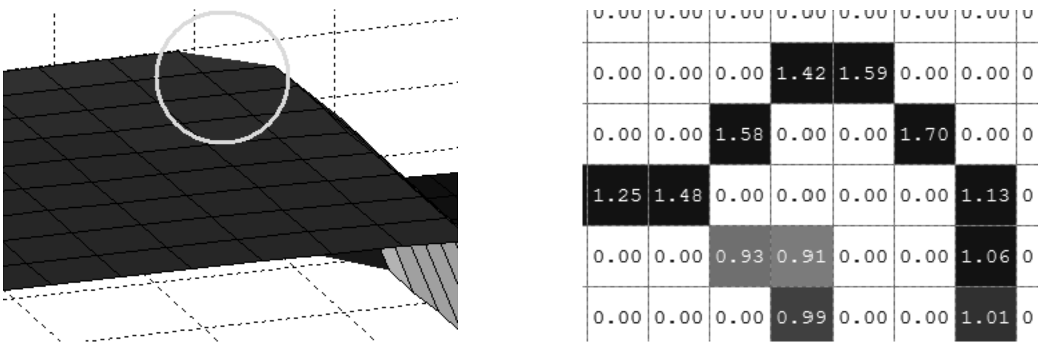

(C) (D)

FIG. 5. Detailed ID_S values for a 2D corner

As expected, the ID for objects which do not vary in distance is equivalent to the one computed in the 2D case.

• In Fig. 5.e the profile for a 3D corner is presented (here, the pixels' intensity varies in all dimensions). The estimated ID_S's for such a corner profile is presented in Fig. 5.f, the value in the target being close to 3, which is the theoretical ID.

• In Fig. 5.g the ID_S's computed for a vertical contour line are presented. We have noticed the ID_S variation, caused by the variation in distance of the contour line (depicted in Fig. 5.h). Hence, the ID is well estimated in this case too, when the theoretical ID is 2 and the variation plane is parallel to the camera plane.

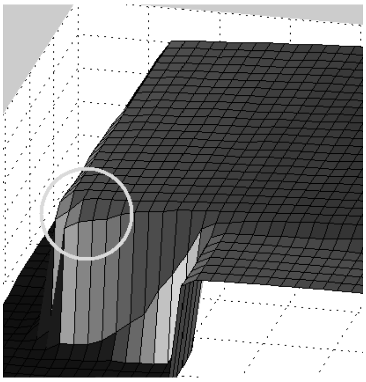

(E)

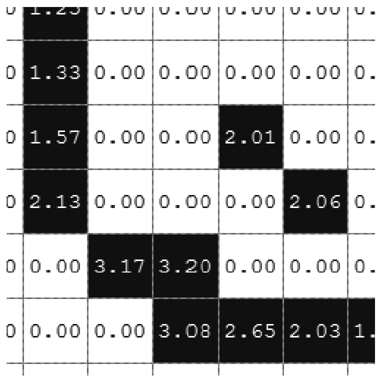

(F)

FIG. 5. Detailed ID_S values for a 3D corner

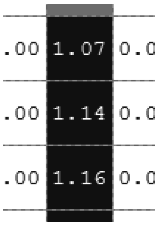

(G)

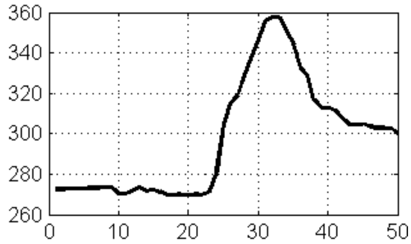

(H)

FIG. 5. a vertical contour line; h) is the distance profile of g)

3.3. Comparison of the ID estimation results for 2D and 3D ToF images

Comparison with respect to the average values for local structures

By comparing 2D versus 3D average ID values (see Tables 2 and 3), one cannot discriminate if one has a 2D or a 3D corner. Hence, in order to discriminate between a 2D and a 3D corner, one has to look at the maximum values within a neighborhood.

Comparison with respect to the point-wise values

As mentioned before, one must focus on the maximum ID values in order to detect pixels defining a local structure. By comparing these values for the two cases, we notice that the 3D values are higher, sometimes much higher (as 7.12 in Table 3 versus 1.78 in Table 1).

The results of estimating the ID on the intensity ToF image are presented in Fig. 4.a, and those on the distance ToF image in Fig. 4.b. The erroneous contours extracted by the Canny extractor are displayed in Fig. 4.a, and they are the result of the image noise and object's non- uniformities. Anyway, one can compare the 2D versus 3D ID estimations. Hence, if we compute the ID_S as for a gray level image by disregarding the distance information (Fig. 4.a and 6.a the maximum ID is 1.04 (as for a low curvature 2D corner); but, if we compute the ID_S as for a 3D

ToF image, by considering also the distance information, the ID is about 3, which reveals the 3D corner from the image.

Table 2

Average values (the $3D$ - ID_S average values obtained for a specified structure in a ToF image)

3D ToF structure	max ID_S	average ID_S
Fig. 5 d)	1.7	1.4
Fig. 5 f)	3.2	2.55

Table 3

Average values (the $3D$ - ID_S average values obtained for a specified structure in an ideal image)

3D structure	max ID_S	average ID_S
	1.75	1.32
	2.06	1.37
	1.75	1.32
	1.27	1.04
	7.12	2.25

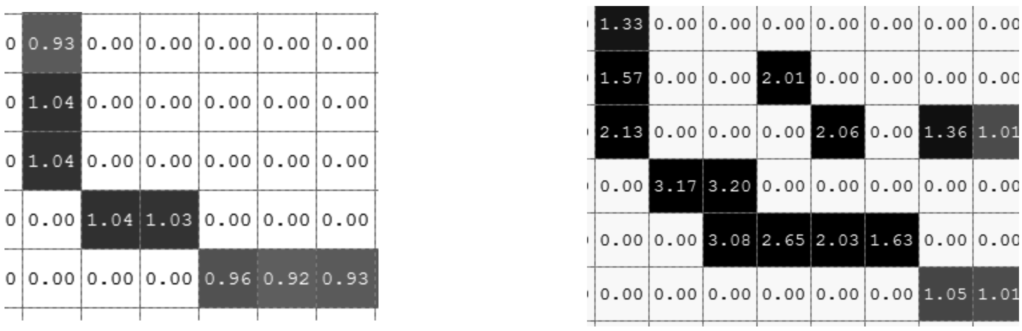

FIG. 6. a) 2D detail; b) 3D detail

Thus, the importance of estimating the ID on the $3D$ image is shown in Fig. 6.b, where ID is close to the theoretical value equal to 3.

4. Conclusions

We proposed a slightly modified definition of ID, allowing to estimate it on the basis of a specified sample S (such as a “contour – sample”)

The MLE constructed for a fixed number of NN-neighbors is recommended when a comparison of ID’s for $2D$ and $3D$ images is of interest.

When using ID_S, identification of the local structures is correct, as this approach works very well for natural, $2D$ images and well enough for ToF $3D$ images.

The quality of the estimate depends on the performances of the contour extractor, due to the involved noise.

One must focus on the maximum ID values in order to detect pixels defining a local structure, and not on the average values for that structure.

The estimated $3D$ ID for objects which do not vary in distance is equivalent to the one computed in the $2D$ case.

The values of ID_S for a $3D$ corner are close to the theoretical value both for $2D$ intensity images and $3D$ distance images.

Acknowledgements

The work has been co-funded by the Sectoral Operational Programme Human Resources Development 2007-2013 of the Romanian Ministry of Labour, Family and Social Protection through the Financial Agreement POSDRU /89/1.5/S/62557. The authors also wishes to thank prof. Erhardt Barth for the very useful discussions related to this research.

REFERENCES

[1] *G. H. Granlund; H. Knutsson*, Signal Processing in Computer Vision, Kluwer Academic Publishers, 1995.

[2] *C. Zetzsche; E. Barth*, Fundamental limits of linear filter in the visual processing of two-dimensional signals, Vision Research 30 (7), p. 1111–1117, 1990, doi:10.1016/0042-6989(90)90120-A

[3] *C, Mota; E. Barth*, On the uniqueness of curvature features, in *Dynamische Perzeption* (series Proceedings in Artificial Intelligence), editor G. Baratoff and H. Neumann, vol 9, p. 175 – 178, Infix Verlag, 2000, http://www.inb.uni-luebeck.de/~barth/papers/ulm2000.html

[4] *T. Aach; C. Mota; I. Stuke; M. Mühlich; E. Barth*, Analysis of Superimposed Oriented Patterns, *IEEE Transactions on Image Processing,* vol 15, 12, p. 3690–3700, 2006, http://www.inb.uni-luebeck.de/publications/pdfs/AaMoStMuBa06.pdf

[5] *C. Mota; I. Stuke; E. Barth*, Analytic solutions for multiple motions, Proc. IEEE Int. Conf. Image Processing, p. 917–920, 2001, http://www.inb.uni-luebeck.de/publications/pdfs/MoStBa01.pdf

[6] *C. Mota; I. Stuke; E. Barth*, The Intrinsic Dimension of Multispectral Images, *MICCAI Workshop on Biophotonics Imaging for Diagnostics and Treatment*, p. 93 - 100, 2006, http://www.inb.uni-luebeck.de/publications/pdfs/MoStBa06.pdf

[7] *M. Felsberg; S. Kalkan; N. Krüger*, Continuous Dimensionality Characterization of Image Structures, Image and Vision Computing vol 27, p. 628–636, 2009

[8] *E. Levina; P.J. Bickel*, Maximum likelihood estimation of intrinsic dimension, Advances in Neural Information Processing Systems, 18, p. 777–784, 2004

[9] *D.J.C. MacKay; Z. Ghahramani*, Comments on 'Maximum likelihood estimation of intrinsic dimension' by E. Levina and P. Bickel, 2005, http://www.inference.phy.cam.ac.uk/mackay/dimension/

[10] *K.M. Carter; R. Raich; A.O. Hero*, On Local Intrinsic Dimension Estimation and Its Applications, IEEE Trans. on Signal Processing, vol.58, no.2, p. 650–663, 2010

[11] *B. Eriksson; M. Crovella*, Estimating intrinsic dimension via clustering, Statistical Signal Processing Workshop (SSP), p. 760–763, 2012

[12] *S. Oprisescu*, Development of systems with tof camera and fusion of 2d/3d sensors for monitoring applications. Technical report, Univ. Politehnica from Bucuresti, Romania, 2010.

[13] *S. Oprisescu, C. Burlacu, and A. Sultana*, A new contour extraction algorithm for tof images. In 10th Int. Symp. on Signals, Circuits and Systems (ISSCS), Iasi, Romania, p. 1–4, 2011.